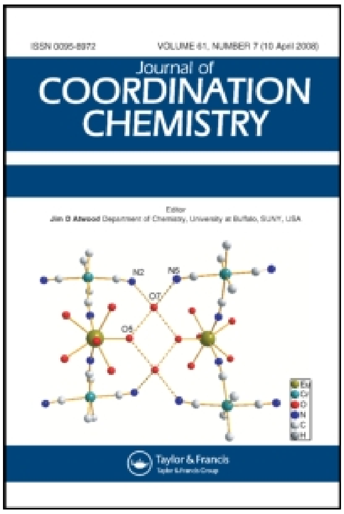

Journal of Coordination Chemistry

Publication details, including instructions for authors and subscription information:
http://www.informaworld.com/smpp/title~content=t713455674

Two new Cu^I(4,5-diazafluoren-9-one)$_2$-modified compounds based on the Keggin anion and its bicapped bisupporting derivative

Xiang-Min Chen[a]; De-Song Wang[a]; Qing-Zhi Luo[a]; Ran Wang[a]
[a] Postgraduate Admissions Office, Hebei University of Science and Technology, Shijiazhuang 050018, P.R. China

To cite this Article Chen, Xiang-Min , Wang, De-Song , Luo, Qing-Zhi and Wang, Ran(2009) 'Two new Cu^I(4,5-diazafluoren-9-one)$_2$-modified compounds based on the Keggin anion and its bicapped bisupporting derivative', Journal of Coordination Chemistry, 62: 24, 3895 — 3904, First published on: 22 September 2010 (iFirst)

To link to this Article: DOI: 10.1080/00958970903261457

URL: http://dx.doi.org/10.1080/00958970903261457

Journal of Coordination Chemistry
Vol. 62, No. 24, 20 December 2009, 3895–3904

Taylor & Francis
Taylor & Francis Group

Two new Cu^I(4,5-diazafluoren-9-one)$_2$-modified compounds based on the Keggin anion and its bicapped bisupporting derivative

XIANG-MIN CHEN*, DE-SONG WANG,
QING-ZHI LUO and RAN WANG

Postgraduate Admissions Office, Hebei University of Science
and Technology, Shijiazhuang 050018, P.R. China

(*Received 6 May 2009; in final form 2 July 2009*)

Two new Cu^I(4,5-diazafluoren-9-one)$_2$-modified compounds based on Keggin anion and its bicapped bisupporting derivative, $[Cu(DF)_2]_3[PMo_{12}O_{40}]$ (**1**), $[Cu(DF)_2]_2[\{PMo_{12}O_{40}(VO)_2\}\{Cu(DF)_2\}_2]$ (**2**) (DF = 4,5-diazafluoren-9-one), have been prepared under hydrothermal conditions and characterized by single-crystal X-ray diffraction, elemental analyses, infrared spectra, thermogravimetric analyses, and cyclic voltammetry. In **1**, the layer consisting of two-coordinate Cu^I complexes arranges alternatively with the other layer consisting of three-coordinate Cu^I complexes. Strong aryl packing interactions between these layers construct a stable supramolecular metal-organic framework with 1D channels, which can accommodate the anions. In **2**, the anion is a reduced bivanadyl capped α-Keggin polymolybdate anion, covalently bonded to two $[Cu(DF)_2]^+$ groups. Chains consisting of $[\{PMo_{12}O_{40}(VO)_2\}\{Cu(DF)_2\}_2]^{2-}$ arrange alternatively with chains consisting of discrete Cu^I complexes. The electrochemical behaviors of carbon paste electrodes for **1** and **2** have been studied in detail.

Keywords: Polyoxometalates; Keggin polyanion; DF complex; Aryl packing

1. Introduction

Polyoxometalates (POMs) possess enormous structural variety and interesting properties leading to applications in topology, catalytic activity, magnetism, photochemistry, and electrochemistry [1–5]. A feature of POMs as inorganic ligands is that they offer multiple potential coordination sites to link metal-organic units. Modifying the surface of POMs with transition-metal complexes (TMCs) is an appealing method to design new structures with improved properties [6, 7]. However, because of the relatively weak coordination ability of POMs, it is still an arduous task to assemble TMC-modified POM-based compounds.

To construct new structures, modifiers (TMCs) are usually adopted selecting the proper organic ligands to tune the coordination environment of the transition-metal ions. Bidentate ligands, such as 1,10-phenanthroline [8–11] and 2,22-bipyridine [12–16]

---

*Corresponding author. Email: chenxm1995@yahoo.com.cn

Journal of Coordination Chemistry
ISSN 0095-8972 print/ISSN 1029-0389 online © 2009 Taylor & Francis
DOI: 10.1080/00958970903261457

with strong coordination capacity gave many new compounds. However, 4,5-diazafluoren-9-one (DF), also a bidentate chelate, has been rarely utilized to modify POMs [17–19]. Until now, there is only one example based on Cu–DF modified Keggin anion $[\mathrm{Cu}_2^{\mathrm{I}}(\mathrm{DF})_2\mathrm{H}_2\mathrm{O}][\mathrm{HPMo}_{10}^{\mathrm{VI}}\mathrm{Mo}_2^{\mathrm{V}}\mathrm{O}_{40}\{\mathrm{Cu}^{\mathrm{II}}(\mathrm{DF})\}]$ [20]. Compared with 1,10-phenanthroline and 2,2′-bipyridine, the distance between N···N atoms in DF is relatively longer (2.6 Å for 1,10-phenanthroline and 2,2′-bipyridine; ~3.0 Å for DF). In this work, we select DF as ligand and Cu ion as transition metal to construct POM-based compounds [21].

Herein, we report two new Cu^{I}(4,5-diazafluoren-9-one)$_2$-modified compounds $[\mathrm{Cu}(\mathrm{DF})_2]_3[\mathrm{PMo}_{12}\mathrm{O}_{40}]$ (**1**) and $[\mathrm{Cu}(\mathrm{DF})_2]_2[\{\mathrm{PMo}_{12}\mathrm{O}_{40}(\mathrm{VO})_2\}\{\mathrm{Cu}(\mathrm{DF})_2\}_2]$ (**2**) (DF = 4,5-diazafluoren-9-one). Compounds **1** and **2** are based on Keggin POM and its bicapped bisupporting derivative, respectively, which give different frameworks.

2. Experimental

2.1. *Materials and methods*

All reagents were of reagent grade and used as received from commercial sources. DF was synthesized [22]. Elemental analyses (C, H, and N) were performed on a Perkin-Elmer 2400 CHN elemental analyzer. Mo and Cu were determined by a Leaman inductively coupled plasma (ICP) spectrometer. IR spectra were obtained on an Alpha Centaurt FT/IR spectrometer with KBr pellets from 400 to 4000 cm^{-1}. The XPS spectrum was recorded on an ESAY ESCA spectrometer with an Mg-Kα achromatic X-ray source. The thermal gravimetric analyses (TGA) were carried out in N_2 on a Perkin-Elmer DTA 1700 differential thermal analyzer with a rate of 10°C min^{-1}. Electrochemical measurements were performed with a CHI 660b electrochemical workstation. A conventional three-electrode system was used. The working electrode was a modified carbon paste electrode (CPE). Ag/AgCl (3 M KCl) electrode was used as a reference electrode and a Pt wire as a counter electrode.

2.2. *Synthesis of $[Cu(DF)_2]_3[PMo_{12}O_{40}]$ (1)*

A mixture of $\mathrm{Na_2MoO_4 \cdot 2H_2O}$ (0.242 g, 1 mmol), $\mathrm{Cu(CH_3COO)_2 \cdot 2H_2O}$ (0.098 g, 0.45 mmol), and DF (0.073 g, 0.4 mmol) was dissolved in 10 mL of distilled water at room temperature. When the pH of the mixture was adjusted to about 4.2 with dilute 1 M $\mathrm{H_3PO_4}$ solution, the suspension was put into a Teflon-lined autoclave and kept under autogenous pressure at 160°C for 4 days. After slow cooling to room temperature, dark red block crystals were filtered and washed with distilled water (40% yield based on Mo). Anal. Calcd for $\mathrm{C_{66}H_{36}Cu_3Mo_{12}N_{12}O_{46}P}$ (%): C, 25.52; H, 1.17; N, 5.41; Mo, 37.07; Cu, 6.14. Found: C, 25.48; H, 1.21; N, 5.35; Mo, 36.96; Cu, 6.08.

2.3. *Synthesis of $[Cu(DF)_2]_2[\{PMo_{12}O_{40}(VO)_2\}\{Cu(DF)_2\}_2]$ (2)*

A mixture of $\mathrm{Na_2MoO_4 \cdot 2H_2O}$ (0.218 g, 0.9 mmol), $\mathrm{Cu(CH_3COO)_2 \cdot 2H_2O}$ (0.087 g, 0.4 mmol), $\mathrm{NH_4VO_3}$ (0.059 g, 0.5 mmol), and DF (0.091 g, 0.5 mmol) was dissolved in 10 mL of distilled water at room temperature. When the pH of the mixture was adjusted to about 4.3 with 1 M H_3PO_4 solution, the suspension was put into a Teflon-lined autoclave and kept under autogenous pressure at 160°C for 4 days. After slow cooling to room temperature, black block crystals were filtered and washed with distilled water (40% yield based on Mo). Anal. Calcd for $C_{88}H_{48}Cu_4Mo_{12}N_{16}O_{50}PV_2$ (%): C, 28.82; H, 1.32; N, 6.11; Mo, 31.39; Cu, 6.93; V, 2.78. Found: C, 28.76; H, 1.35; N, 6.07; Mo, 31.29; Cu, 6.87; V, 2.70.

2.4. *X-ray crystallography*

X-ray diffraction analysis data for **1** and **2** were collected on a Rigaku RAXIS RAPID IP with Mo-Kα monochromatic radiation ($\lambda = 0.71073$ Å) at 293 K. The structures were refined by full-matrix least-squares on F^2 using the SHELXTL crystallographic software package [23]. All hydrogens attached to carbon were generated geometrically. The crystal and structure refinement data for **1** and **2** are summarized in table 1. Selected bond lengths (Å) and angles (°) are listed in table 2. CCDC 707424 for **1** and 707425 for **2** contain the supplementary crystallographic data for this article.

2.5. *Preparations of 1- and 2-CPEs*

The compound **1** modified CPE (**1**-CPE) was fabricated as follows: 90 mg of graphite powder and 8 mg of **1** were mixed and ground together by an agate mortar and pestle to achieve a uniform mixture, and then 0.1 mL of Nujol was added with stirring. The homogenized mixture was packed into a glass tube with a 1.5 mm inner diameter, and the tube surface was wiped with paper. Electrical contact was established with a copper rod through the back of the electrode. In a similar manner, **2**-CPE was made.

Table 1. Crystal data and structure refinement for **1** and **2**.

Empirical formula	$C_{66}H_{36}Cu_3Mo_{12}N_{12}O_{46}P$	$C_{88}H_{48}Cu_4Mo_{12}N_{16}O_{50}PV_2$
Formula weight	3105.9	3667.7
Temperature (K)	293(2)	293(2)
Crystal system	Triclinic	Triclinic
Space group	$P\bar{1}$	$P\bar{1}$
Unit cell dimensions (Å, °)		
a	10.663(2)	11.851(2)
b	13.592(3)	13.555(3)
c	14.847(3)	16.596(3)
α	87.45(3)	104.58(3)
β	75.87(3)	95.56(3)
γ	77.18(3)	96.33(3)
Volume (Å^3), Z	2034.7(7), 1	2542.9(9), 1
Calculated density (g cm^{-3})	2.534	2.395
Absorption coefficient (mm^{-1})	2.676	2.537
Final R indices [$I > 2\sigma(I)$]	$R_1{}^a = 0.0784$, $wR_2{}^b = 0.1703$	$R_1{}^a = 0.0798$, $wR_2{}^b = 0.1976$
R indices (all data)	$R_1{}^a = 0.0900$, $wR_2{}^b = 0.1758$	$R_1{}^a = 0.0942$, $wR_2{}^b = 0.2059$
Goodness-of-fit on F^2	1.052	0.999
Largest difference peak and hole (e Å^{-3})	1.758 and −1.599	3.598 and −2.183

${}^{a}R_1 = \Sigma||F_o| - |F_c||/\Sigma|F_o|$. ${}^{b}wR_2 = \{\Sigma[w(F_o^2 - F_c^2)^2]/\Sigma[w(F_o^2)^2]\}^{1/2}$.

Table 2. Selected bond lengths (Å) and angles (°) for **1** and **2**.

1			
Cu(1)–N(1)	1.885(11)	Cu(1)–N(1)#2	1.885(11)
Cu(2)–N(5)	1.856(15)	Cu(2)–N(3)	1.872(15)
Cu(2)–N(4)	2.678(16)	Cu(2)′–N(5)	2.10(12)
Cu(2)′–N(3)	2.205(15)	Cu(2)′–N(4)	2.053(16)
N(3)–Cu(2)–N(4)	76.71(5)	N(1)–Cu(1)–N(1)#2	180.0(11)
N(5)–Cu(2)–N(3)	162.38(6)	N(5)–Cu(2)–N(4)	115.45(6)
N(3)–Cu(2)′–N(4)	85.54(5)	N(5)–Cu(2)–N(3)	121.81(6)
N(5)–Cu(2)–N(4)	143.58(6)	O(8)–Mo(6)–O(12)#1	100.7(8)
2			
Cu(1)–N(3)	1.907(13)	Cu(1)–N(2)	1.911(12)
Cu(1)–O(4)	2.286(12)	Cu(2)–N(8)	1.953(18)
Cu(2)–N(5)	1.94(2)	Cu(2)–N(7)	2.616(2)
Cu(2)–N(6)	2.63(3)	V(1)–O(19)	1.959(10)
V(1)–O(18)	1.931(11)	V(1)–O(21)	1.958(10)
V(1)–O(20)	1.940(10)	N(3)–Cu(1)–N(2)	167.8(6)
V(1)–O(4)	1.600(11)	N(2)–Cu(1)–O(4)	95.0(5)
N(3)–Cu(1)–O(4)	97.2(5)	N(6)–Cu(2)–N(7)	165.07(2)
N(5)–Cu(2)–N(8)	165.2(7)	O(15)–Mo(2)–O(21)#1	100.0(6)

Symmetry codes for **1**: #1 $-x, -y+1, -z+1$; #2 $-x-1, -y, -z+1$. **2**: #1 $-x+1, -y+3, -z-1$.

3. Results and discussion

3.1. *Synthesis*

Compounds **1** and **2** were synthesized under identical hydrothermal conditions except for adding NH_4VO_3 for **2**, which can reduce to different structures. In **1**, the inorganic building block is $[PMo_{12}O_{40}]^{3-}$ (abbreviated to PMo_{12}), while in **2** is its bicapped bisupporting derivative $\{PMo_{12}O_{40}(VO)_2\}^{+}$ (abbreviated to $PMo_{12}V_2$). The different anions induce different frameworks. Furthermore, the oxidation state of copper changes from Cu^{II} to Cu^{I}, while vanadium changes from V^{V} to V^{IV}. DF acts as ligand and reducing agents. Such a phenomenon is often observed in a hydrothermal reaction system containing N-donor ligand, Cu^{II} and V^{V} [24–26].

3.2. *Crystal structure of 1*

Single-crystal X-ray structural analysis reveals that **1** consists of one α-Keggin anion PMo_{12}, three Cu^{I} ions and six DF ligands (figure 1). The valence sum calculations [27] and XPS spectra show that all Mo atoms are in +VI oxidation state, while Cu atoms are in +I. In PMo_{12} anion, each molybdenum has a distorted $\{MoO_6\}$ octahedral environment with Mo–O distances in the range 1.637(12)−2.536(11) Å. The central P is surrounded by a cube of eight oxygens, with each oxygen site half-occupied. The P–O average distance is 1.525(13) Å.

In **1**, copper ions have two coordination modes: (i) Cu1 adopts linear geometry, coordinated by two nitrogens from two DF ligands. The bond distances and angles around Cu1 are 1.885(11) Å for Cu–N and 180.0(11)° for N–Cu–N. (ii) Cu2 adopts T-shaped geometry, coordinated by three nitrogens from two DF ligands. The bond distances and angles around the Cu2 are 1.856(15)−2.678(16) Å for Cu–N and 76.71(5)−162.38(6)° for N–Cu–N. The closest Cu2···N6 (2.861(2) Å), Cu2′···N6

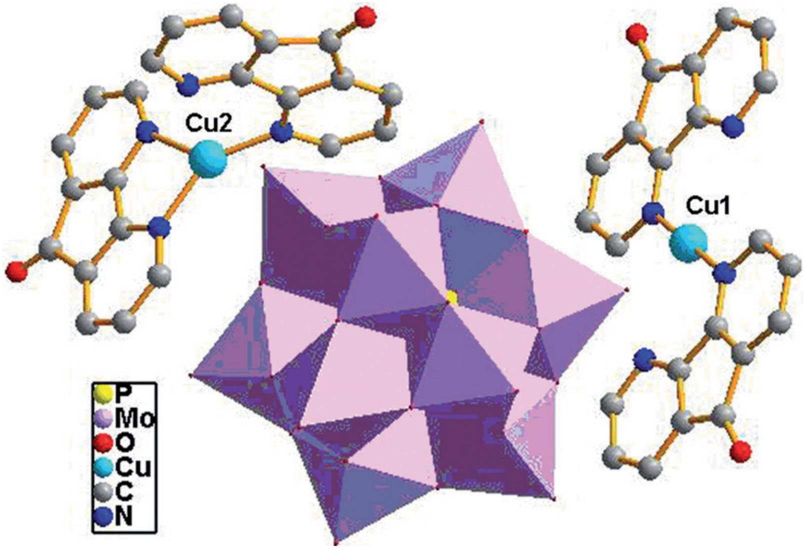

Figure 1. Polyhedral and ball/stick view of **1**. Hydrogens are omitted for clarity.

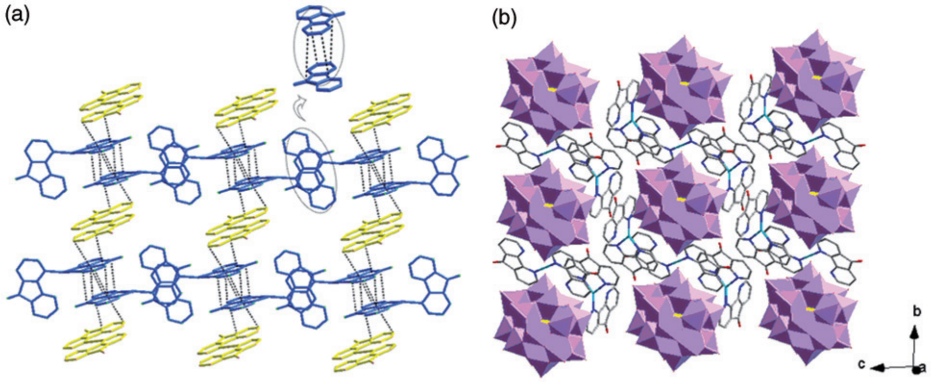

Figure 2. (a) Strong aryl packing interactions between DF ligands induce a stable supramolecular metal-organic framework with 1D channels in **1**. (b) The anions imbed in these channels.

(2.794(3) Å) and Cu1 $\cdots$ N2 (2.917(6) Å) can be treated as strong short contact interactions. The DFs in **1** show two coordination modes, monodentate, and chelate bidentate.

There are two discrete copper complexes $[Cu(DF)_2]^+$ in **1**. In the Cu1 complex, two DF ligands are in one plane. However, in Cu2 complex, the two DF ligands are vertical to each other. The layer consisting of Cu1 complexes arranges alternatively with the other layer consisting of Cu2 complexes (figure 2a). There exist strong face-to-face aromatic–aromatic interactions between DF molecules, which can be viewed as an important factor for stabilizing the metal-organic supramolecular framework. The $\pi \cdots \pi$ stacking distances between the corresponding DF molecules vary from 3.302 to 3.373 Å. This packing mode of these metal-organic complexes gives a 1D channel structure (figure S1) which can accommodate the Keggin anions (figure 2b). The anion has abundant hydrogen bonding interactions with Cu–DF complexes. For example, the short C–H ⋯ O distances between DF and oxygen of the Keggin anion are C(11)–H(11) ⋯ O(7): 2.26(2) Å, C(21)–H(21) ⋯ O(17): 2.42(3) Å, C(2)–H(2) ⋯ O(8): 2.43(4) Å, and C(32)–H(32) ⋯ O(17): 2.50(2) Å. Therefore, both the aryl packing and hydrogen bonding interactions make **1** stable.

3.3. *Crystal structure of 2*

Single-crystal X-ray structural analysis reveals that **2** consists of one bicapped bisupporting derivative $PMo_{12}V_2$, four Cu^I ions and eight DF ligands (figure 3). The valence sum calculations [27] and XPS spectra show that five Mo atoms are in the +V oxidation state, while coppers are all in the +I oxidation state and V are +IV. The inorganic building block $PMo_{12}V_2$ is built on the classical α-Keggin structure with $\{VO\}_2$ covering four bridging oxygens from corner-sharing adjacent Mo_3O_{13} trimetallic clusters. The τ factor ($\tau = (\beta - \alpha)/60$) [28] of V is 0.03, an index of the degree of trigonality within the structural continuum between trigonal bipyramidal and square pyramidal. The result indicates that $\{VO_5\}$ is a square pyramid. In **2**, the P–O average distance is 1.516(11) Å. The Mo–O bond lengths are in the range 1.615(11)–2.52(2) Å and V–O in the range 1.600(11)–1.931(11) Å.

Cu1 is three coordinate by two nitrogens from two DF ligands and one O from $PMo_{12}V_2$ anion, adopting T-shaped geometry. The bond distances and angles around Cu1 are 1.907(13) and 1.911(12) Å for Cu–N, 2.286(12) Å for Cu–O and 167.8(6)° for N–Cu–N. Cu2 adopts rectangle geometry, coordinated by four nitrogens from two DF ligands. Bond distances and angles around Cu1 are 1.94(2)–2.63(3) Å for Cu–N and

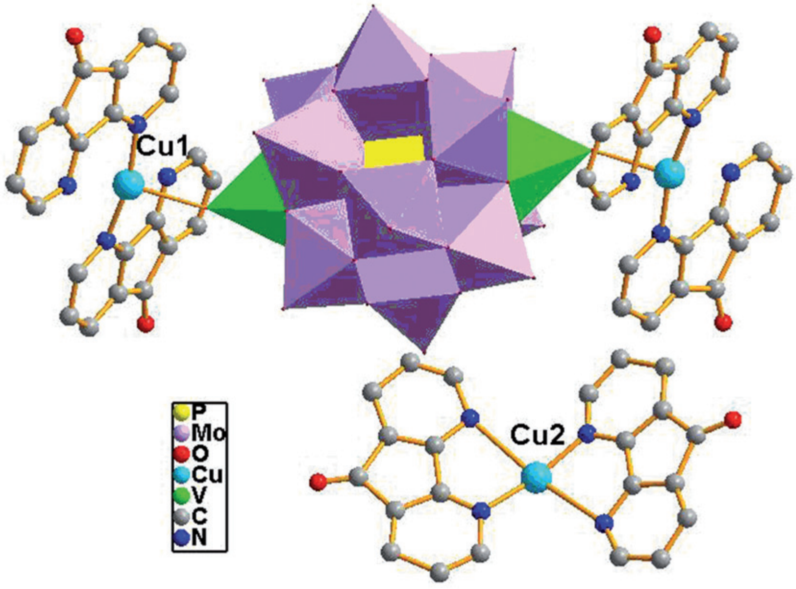

Figure 3. Polyhedral and ball/stick view of **2**. Hydrogens are omitted for clarity.

79.85(11)–165.2(7)° for N–Cu–N. In comparison with **1**, the DF molecules in **2** also show two coordination modes, monodentate, and chelate bidentate.

In **2**, two Cu1–DF complexes are grafted covalently to one $PMo_{12}V_2$ anion through two terminal O4s from opposite capping {VO} groups to form a bicapped bisupporting cluster. Each cluster joins other neighboring ones through $\pi \cdots \pi$ stacking interactions between DF molecules, constructing a supramolecular chain. Discrete Cu2 complexes connect with each other through $\pi \cdots \pi$ stacking and hydrogen bonding interactions to construct the supramolecular chain. The short distances of C–H $\cdots$ O between Cu2 and oxygen of the POM anion are C(35)–H(35A) $\cdots$ O(10): 2.50(2) Å, C(35)–H(35A) $\cdots$ O(7): 2.51(3) Å, C(43)–H(43A) $\cdots$ O(13): 2.51(5) Å, and C(32)–H(32A) $\cdots$ O(13): 2.62(2) Å. These two kinds of chains further arrange alternatively through hydrogen bonds to form a 2D supramolecular layer (figure 4). The $\pi \cdots \pi$ stacking interaction distances between corresponding DF molecules vary from 3.455 to 3.713 Å.

3.4. *FT-IR spectra, XPS spectra, and TG analyses*

Infrared (IR) spectra (figure S2) exhibit the characteristic bands of the α-Keggin structure at 939, 867, 791, 1048 cm^{-1} for **1** and 944, 859, 780, 1048 cm^{-1} for **2**, attributed to $\nu(M–O_t)$, $\nu(M–O_b–M)$, $\nu(M–O_c–M)$ (M = V or Mo), and ν(P–O). Bands at 1396–1728 cm^{-1} for **1** and 1405–1732 cm^{-1} for **2** are characteristics of DF.

The X-ray photoelectron spectroscopy (XPS) spectra show peaks at 233 and 236.1 eV for **1** attributed to $Mo^{6+}(3d_{5/2})$ and $Mo^{6+}(3d_{3/2})$, while two overlapped peaks at 232.9

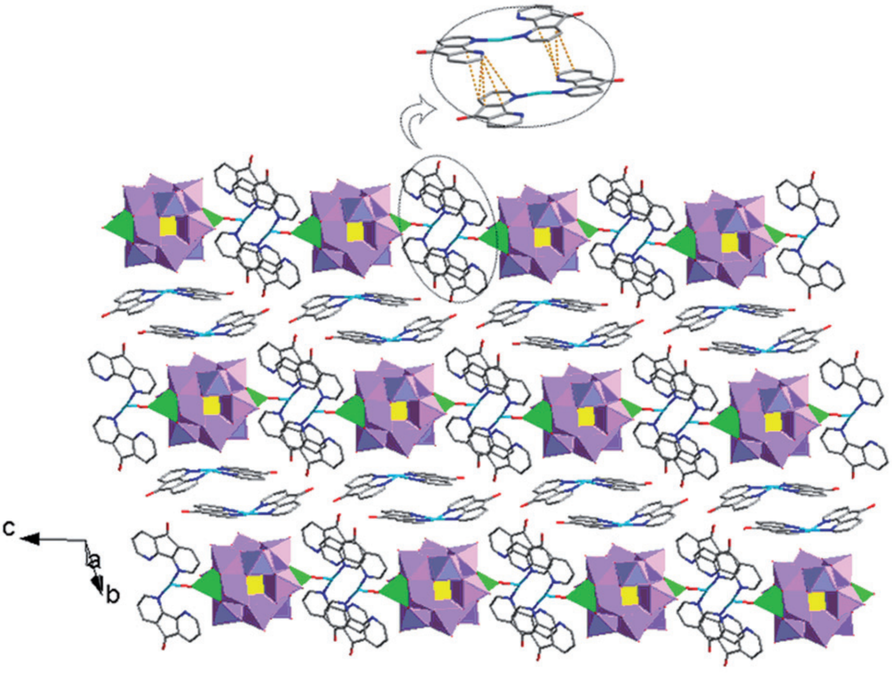

Figure 4. In **2**, the chains composed of $[\{PMo_{12}O_{40}(VO)_2\}\{Cu(DF)_2\}_2]^{2-}$ arrange alternatively with the chains composed of discrete Cu2 complexes. There exist abundant aryl packing interactions between DF molecules.

and 231.8 eV for **2** are attributed to Mo_{3d}^{6+} and Mo_{3d}^{5+}. Two peaks at 932.4 and 952.4 eV for **1**, 931.1 and 950.9 eV for **2** are attributed to $Cu^+(2p_{3/2})$ and $Cu^+(2p_{5/2})$. A peak at 515.8 eV for **2** can be attributed to V(IV) (figures S3 and S4).

TGA experiments were performed under N_2 with a heating rate of 10°C min^{-1} from 40−650°C. In TG curves, the weight loss steps (figure S5) of both **1** and **2** may be ascribed to decomposition of all DF molecules, giving total loss of 36.67% (Calcd 36.73%) for **1** and 39.57% (Calcd 39.28%) for **2**.

3.5. *Voltammetric behaviors of 1-, 2-CPEs in aqueous electrolyte*

Compounds **1** and **2** are insoluble in water and common organic solvents and bulk-modified CPE becomes the optimal choice to study their electrochemical properties [29, 30]. **1**- and **2**-CPE exhibit similar voltammetric behavior in aqueous electrolyte, except for some slight potential shifts of the redox peaks (Supplementary material). The redox wave of V^V/V^{IV} in **2**-CPE is not observed in the scan range +800 and −240 mV, as observed for other P/Mo/V systems [25, 31]. Owing to the similarity of electrochemical behavior for these two CPEs, only cyclic voltammograms for **1**-CPE at different scan rates in the potential range +1000 to −180 mV are described here. There exist three reversible redox peaks I–I′, II–II′, III–III′ with the half-wave potentials $E_{1/2} = (E_{pa} + E_{pc})/2$ at +400 (I–I′), +249 (II–II′) and −6 (III–III′) mV (scan rate: 100 mV s^{-1}), respectively, attributed to three consecutive two-electron processes of the Mo(VI/V) couples [20, 32–34]. Furthermore, when the scan rates varied from 20 to 340 mV s^{-1} for **1**-CPE, the peak potentials change gradually with cathodic peak potentials shifting negative and the corresponding anodic peak potentials positive with increasing scan rates. The results verify that the redox ability of the parent α-Keggin anion can be maintained in the hybrid solids, indicating application of this kind of inorganic–organic hybrid materials in electrochemistry.

3.6. *Electrocatalytic reduction of bromate and nitrite on 1-CPE*

Cyclic voltammograms for the electrocatalytic reduction of bromate at the **1**-CPE in 1 M H_2SO_4 aqueous solution are provided as "Supplementary material". At **1**-CPE, with the addition of bromate, the third reduction peak currents increase gradually while the corresponding oxidation peak currents gradually decrease, while the first two redox peaks remain almost unchanged, indicating that the six-electron reduced species of PMo_{12} anions are electrocatalytically active for the reduction of bromate. Electrocatalytic reductions of nitrite by a **1**-CPE in 1 M H_2SO_4 aqueous solution show that with addition of nitrite, all three reduction peak currents gradually increase while the corresponding oxidation peak currents decrease, suggesting that nitrite is reduced by two-, four-, and six-electron reduced species of PMo_{12} anions.

4. Conclusion

Two new compounds based on Keggin and its bicapped bisupporting derivative have been prepared under hydrothermal conditions. The ligand 4,5-diazafluoren-9-one has been rarely utilized to modify POMs. In **1**, the strong aryl packing interactions between

DF ligands construct a stable supramolecular metal-organic framework with 1D channels, which accommodate the anions. In **2**, chains consisting of $[\{PMo_{12}O_{40}(VO)_2\}\{Cu(DF)_2\}_2]^{2-}$ arrange alternatively with the chains consisting of discrete Cu2 complexes. Compared with other bidentate chelate ligands, the DF molecule exhibits abundant coordination modes, extending the field of TMCs-modified POM-based compounds. The choice of DF offers new target synthesis. Ongoing efforts are focused on the choice of organic ligands and transition metal to obtain new POM-based compounds.

Supplementary material

The data for compounds **1** and **2** can be obtained free of charge from The Cambridge Crystallographic Centre *via* www.ccdc.cam.ac.uk/data-request/cif.

Acknowledgment

This work was financially supported by the Doctoral Research Fund for Hebei Higher Learning Institutions (05547004D-1).

References

[1] K. Kamata, S. Yamaguchi, M. Kotani, K. Yamaguchi, N. Mizuno. *Angew. Chem. Int. Ed.*, **47**, 2407 (2008).

[2] S.T. Zheng, J. Zhang, G.Y. Yang. *Angew. Chem. Int. Ed.*, **47**, 3909 (2008).

[3] W.L. Huang, M. Schopfer, C. Zhang, R.C. Howell, L. Todaro, B.A. Gee, L.C. Francesconi, T. Polenova. *J. Am. Chem. Soc.*, **130**, 481 (2008).

[4] M. Nyman, C.R. Powers, F. Bonhomme, T.M. Alam, E.J. Maginn, D.T. Hobbs. *Chem. Mater.*, **20**, 2513 (2008).

[5] A.M. Douvas, E. Makarona, N. Glezos, P. Argitis, J.A. Mielczarski, E. Mielczarski. *ACS Nano*, **2**, 733 (2008).

[6] C. Streb, C. Ritchie, D.L. Long, P. Kögerler, L. Cronin. *Angew. Chem., Int. Ed.*, **46**, 7579 (2007).

[7] J.W. Zhao, C.M. Wang, J. Zhang, S.T. Zheng, G.Y. Yang. *Chem. Eur. J.*, **14**, 9223 (2008).

[8] V. Shivaiah, S.K. Das. *Inorg. Chem.*, **44**, 8846 (2005).

[9] C.M. Liu, J.L. Luo, D.Q. Zhang, N.L. Wang, Z.J. Chen, D.B. Zhu. *Eur. J. Inorg. Chem.*, 4774 (2004).

[10] C.Y. Sun, Y.G. Li, E.B. Wang, D.R. Xiao, H.Y. An, L. Xu. *Inorg. Chem.*, **46**, 1563 (2007).

[11] M.X. Li, G.L. Guo, J.Y. Niu. *J. Coord. Chem.*, **61**, 3860 (2008).

[12] R.G. Cao, S.X. Liu, L.H. Xie, Y.B. Pan, J.F. Cao, Y.H. Ren, L. Xu. *Inorg. Chem.*, **46**, 3541 (2007).

[13] C. Ritchie, E. Burkholder, P. Kögerler, L. Cronin. *J. Chem. Soc., Dalton Trans.*, 1712 (2006).

[14] C.M. Wang, S.T. Zheng, G.Y. Yang. *Inorg. Chem.*, **46**, 616 (2007).

[15] X.J. Wang, X.M. Lu, P.Z. Li, X.H. Pei, C.H. Ye. *J. Coord. Chem.*, **61**, 3753 (2008).

[16] W.L. Chen, Y.H. Wang, Y.G. Li, E.B. Wang, Y.W. Li. *J. Coord. Chem.*, **62**, 1035 (2009).

[17] P. Kulkarni, S. Padhye, E. Sinn. *Inorg. Chim. Acta*, **321**, 193 (2001).

[18] B.L. Li, B.Z. Li, X. Zhu, Y. Zhang. *Inorg. Chem. Commun.*, **6**, 1304 (2003).

[19] B.L. Wu, H.Y. Zhang, Q.A. Wu, H.W. Hou, Y. Zh. *J. Mol. Struct.*, **655**, 467 (2003).

[20] A.X. Tian, Z.G. Han, J. Peng, J. Ying, J.Q. Sha, B.X. Dong, J.L. Zhai, H.S. Liu. *Inorg. Chim. Acta*, **361**, 1332 (2008).

[21] A.X. Tian, J. Ying, J. Peng, J.Q. Sha, Z.G. Han, J.F. Ma, Z.M. Su, N.H. Hu, H.Q. Jia. *Inorg. Chem.*, **47**, 3274 (2008).

[22] L.J. Henderson, F.R. Fronczek, W.R. Cherry. *J. Am. Chem. Soc.*, **106**, 5876 (1984).

[23] (a) G.M. Sheldrick. *SHELXTL-97, Program for Crystal Structure Solution*, University of Göttingen, Göttingen, Germany (1997); (b) G.M. Sheldrick. *SHELXTL-97, Program for Crystal Structure Refinement*, University of Göttingen, Göttingen, Germany (1997).
[24] C.M. Liu, D.Q. Zhang, D.B. Zhu. *Cryst. Growth Des.*, **6**, 524 (2006).
[25] Z.Y. Shi, J. Peng, C.J. Gómez-García, S. Benmansour, X.J. Gu. *J. Solid State Chem.*, **179**, 253 (2006).
[26] A.X. Tian, Z.G. Han, J. Peng, J.Q. Sha, Y.L. Zhao, H.J. Pang, P.P. Zhang, M. Zhu. *Solid State Sci.*, **10**, 1352 (2008).
[27] I.D. Brown, D. Altermatt. *Acta Crystallogr. B*, **41**, 244 (1985).
[28] A.W. Addison, T.N. Rao, J. Reedijk, J. Rijn, G.C. Verschoor. *J. Chem. Soc., Dalton Trans.*, **7**, 1349 (1984).
[29] X.L. Wang, H. Zhang, E.B. Wang, Z.B. Han, C.W. Hu. *Mater. Lett.*, **58**, 1661 (2004).
[30] Z.G. Han, Y.L. Zhao, J. Peng, Y.H. Feng, J.N. Yin, Q. Liu. *Electroanalysis*, **17**, 1097 (2005).
[31] Z.Y. Shi, X.J. Gu, J. Peng, Y.H. Chen. *J. Solid State Chem.*, **178**, 1988 (2005).
[32] M. Sadakane, E. Steckhan. *Chem. Rev.*, **98**, 219 (1998).
[33] P. Wang, X.P. Wang, X.Y. Jing, G.Y. Zhu. *Anal. Chim. Acta*, **424**, 51 (2000).
[34] X.L. Wang, C. Qin, E.B. Wang, Z.M. Su, Y.G. Li, L. Xu. *Angew. Chem. Int. Ed.*, **45**, 7411 (2006).